Published in final edited form as:

J Neurochem. 2008 July ; 106(1): 83–95. doi:10.1111/j.1471-4159.2008.05348.x.

D_2 dopamine receptor expression and trafficking is regulated through direct interactions with ZIP

Ok-Jin Kim[*], **Marjorie A. Ariano**[†], **Yoon Namkung**[‡], **Paul Marinec**[‡], **Eunmi Kim**[‡], **Jian Han**[‡], and **David R. Sibley**[‡]

[*]Department of Pharmacology and Toxicology, School of Pharmacy, University of Kansas, Lawrence, Kansas, USA

[†]Department of Neuroscience, The Chicago Medical School at Rosalind Franklin University of Medicine and Science, North Chicago, Illinois, USA

[‡]Molecular Neuropharmacology Section, National Institute of Neurological Disorders and Stroke, National Institutes of Health, Bethesda, Maryland, USA

Abstract

We have used the yeast two-hybrid system to identify protein kinase C-ζ interacting protein (ZIP) as a novel interacting protein for the D_2 dopamine receptor (DAR). This interaction was identified by screening a rat brain cDNA library using the third intracellular loop of the D_2 DAR as bait. A partial-length cDNA encoding ZIP was isolated and characterized as specifically interacting with the third intracellular loop of the D_2 DAR, but not with the third intracellular loops of other DAR subtypes. Biochemical confirmation of the ZIP–D_2 DAR interaction was obtained by expressing the full-length ZIP and D_2 DAR proteins in mammalian cells and demonstrating that they could be co-immunoprecipitated. We further showed that ZIP and the D_2 DAR could be co-immunoprecipitated from endogenous brain tissues. Immunohistochemical analyses further revealed that ZIP and the D_2 DAR were extensively co-localized within numerous neurons in various brain regions. ZIP exists as three protein isoforms of varying length, which are derived from alternative RNA splicing. All three isoforms were found to interact with the D_2 DAR, which allowed for the delineation of the receptor interacting domain to within 38 residues of ZIP. Functionally, over-expression of ZIP was found to result in decreased expression of the D_2 DAR with a corresponding decrease in receptor modulation of cAMP accumulation. Confocal microscopy revealed that ZIP over-expression also lead to an intracellular accumulation of D_2 DAR protein in lysosome compartments. These results suggest that ZIP can physically interact with the D_2 DAR leading to increased intracellular trafficking to lysosomes with subsequent down-regulation of receptor expression and function.

Keywords

D_2 dopamine receptor; interacting protein; lysosomes; protein kinase C-ζ interacting protein; trafficking

---

Address correspondence and reprint requests to Dr Ok-Jin Kim, Department of Pharmacology and Toxicology, School of Pharmacy, University of Kansas, 5060 Malott Hall, 1251 Wescoe Hall Dr Lawrence, KS 66045-7582, USA. jokim@ku.edu.

The neurotransmitter dopamine (DA) plays a prominent role in various brain functions including motor control, emotional response, attention, and reward. Abnormal activity of the DA system has been implicated in psychological and neurological disorders, including Parkinson's disease, schizophrenia, mood disorders, addiction, attention deficit hyperactivity disorder, and Tourette's syndrome. The activity of DA and DA congeners is mediated through a family of structurally related seven transmembrane G protein-coupled receptors. Dopamine receptors (DARs) have two subfamilies, the D_1-like DARs (D_1 and D_5) and the D_2-like DARs (D_2, D_3, and D_4). This classification is based on their functional, structural, and pharmacological characteristics (reviewed in Missale *et al.* 1998; Neve *et al.* 2004). The D_1-like DARs stimulate adenylate cyclase through G_s or G_{olf} proteins and have short third cytoplasmic loops (IC3) and long carboxyl terminal cytoplasmic tails. The D_2-like DARs have long IC3 and short carboxyl terminal cytoplasmic tails, and signal through multiple pathways, including inhibition of adenylate cyclase, inhibition of Ca^{2+} channels, activation of K^+ channels, and potentiation of arachidonic acid release.

Besides G proteins, many other proteins are also believed to directly interact with DAR subtypes to regulate their signaling and function. Indeed, a number of novel dopamine receptor interacting proteins (DRIPs) have recently been identified that are not members of the G protein family (reviewed in Bergson *et al.* 2003; Kabbani and Levenson 2007). The precise roles of the various DRIPs identified thus far are still being elucidated; however, preliminary investigations have revealed multiple roles in regulating expression, trafficking, signaling, or localization of the receptors.

In the present study, we use the yeast two-hybrid (Y2H) approach to identify protein kinase Cζ (PKCζ) interacting protein (ZIP) as a novel interacting protein for the D_2 DAR. ZIP was originally isolated from a rat brain cDNA library (Puls *et al.* 1997) and is highly homologous to human p62 (Joung *et al.* 1996) and also to A170, a gene induced by oxidative stress in mouse macrophages (Ishii *et al.* 1996). ZIP undergoes alterative RNA splicing to yield three variants: a full-length ZIP1 as well as two shorter variants, ZIP2 and ZIP3. ZIP1 and ZIP2 were both isolated from screening a rat hippocampal cDNA library using a Kvβ2 potassium channel subunit (Gong *et al.* 1999). ZIP2 is 27 amino acids shorter than ZIP1. ZIP3 was identified as an interacting protein for the $GABA_C$ receptor ρ3 subunit and at 234 amino acids in length is 205 residues shorter than ZIP1 (Croci *et al.* 2003). ZIP3 has been shown to heteromerize with other ZIP family members and to directly interact with the $GABA_C$ receptor, PKCζ and the Kvβ2 potassium channel subunit *in vitro* (Croci *et al.* 2003). We now find that all three splice variants of ZIP interact with the D_2 DAR and that ZIP1 is co-localized with the D_2 DAR within striatal and cortical neurons. The functional consequence of ZIP–D_2 interactions is to reduce receptor expression on the cell surface via enhanced trafficking of the receptors to lysosomes, resulting in degradation. ZIP thus appears to be an important regulator of D_2 DAR mediating signaling in the brain.

Materials and methods

Materials

A rat whole brain cDNA library was purchased from Origene Technologies Inc. (Rockville, MD, USA). Synthetic media for yeast cell culture and yeast isolation system were purchased from Bio101 Inc. (Vista, CA, USA). The calcium–phosphate precipitation kit for transfection was purchased from Clontech (Mountain View, CA, USA). Bicinchoninic acid (BCA) protein assay and Super signal DURA and PICO chemiluminescent substrates were purchased from Pierce (Rockford, IL, USA). Complete protease inhibitor cocktail was purchased from (Roche Diagnostic Corp., Indianapolis, IN, USA). Ezview red anti-FLAG (octapeptide epitope) affinity agarose and protein G affinity agarose, anti-FLAG antisera conjugated with horseradish peroxidase (HRP), forskolin, Ro-20–1724, (+)-Butaclamol, propranolol, DA, sodium metabisulfite, and perchloric acid were purchased from Sigma (St Louis, MO, USA). Anti-Myc-HRP, anti-HA-HRP, and anti-ZIP antisera were obtained from Santa Cruz Biotechnology Inc. (Santa Cruz, CA, USA). Anti-D_2 DAR was a product of Chemicon (Millipore, Billerica, MA, USA) and Cy2 and Cy3 antisera were from Jackson ImmunoResearch (West Chester, PA, USA). [^{3}H]methylspiperone and [^{3}H]SCH 23390 were purchased from Perkin Elmer Life and Analytical Science (Shelton, CT, USA); [^{32}P]H_3PO_4 was from Amhersham Corp. (Arlington Heights, IL, USA). LysoTracker Red was from Invitrogen (Carlsbad, CA, USA).

Plasmid construction and cDNA library screening

The yeast strain EGY48 was purchased from Display Systems Biotech (Vista, CA, USA). The third cytoplasmic domain of the rat D_2 DAR (amino acids Leu211–Gln374) was amplified by PCR using the sense primer 5′-TCAAAATCTACATCGTCCTCCG-GAAG-3′ containing a *Bam*H1 site and the antisense primer 5′-CTGAGTGGCTTTCTTCTCCTTCTG-3′ containing an *Xho*1 site. This amplified PCR product was subcloned in-frame into the *Bam*H1 and *Xho*1 sites of the yeast expression vector pEG202 resulting in plasmid pEG202-D_2^{3rd} encoding the LexA-D_2^{3rd} fusion protein. The third cytoplasmic domains of the D_1, D_3, D_4, and D_5 DARs were amplified by PCR using the sense primers: 5′-GTATCTACAGGATTGCCCAGAAGC-3′, 5′-CCAGGATCTACA-TAGTCCTGAGGCAAA-3′, 5′-TGGGCCACTTTCCGTGGCTTG-CGGCG-3′, and 5′-GTATCTACCGCATTGCGCAGGTGCAG-3′, respectively, all containing a *Bam*H1 site, and the antisense primers: 5′-GCGTCTTTAGAACTTTCGTCTCCC-3′, 5′-CTGGGTGGCCT-TCTTCTCTCGAAGTGG-3′, 5′-CTCATCGCCTTGCGCTCCCTT-CCAGTG-3′, and 5′-TTTGAAGACCTTGGTCTCCTTCTTGAT-3′, respectively, all containing an *Xho*1 site. The individual PCR products were subcloned in-frame into the *Bam*H1 and *Xho*1 sites of the yeast expression vector pEG202 encoding the LexA fusion protein. The yeast expression vectors containing the truncated forms of the third cytoplasmic domain of the D_2 DAR referred as T0, T1, and T2, were generated using the sense primers, 5′-TCAAAATC-TACATCGTCCTCCGGAAG-3′ containing a *Bam*H1 site, and the antisense primers, 5′-GAGTGGTGTCTTCAGGTTGGCTC-3′ and 5′-ATCCATTCTCCGCCTGTTCACTG-3′, 5′-GGATGGATCAGG-GAGAGTGA-3′, respectively, containing an *Xho*1 site. A rat whole brain cDNA library was subcloned into pJG4.5. Two-hybrid techniques (DupLex-A system, Origene Technologies Inc., Rockville, MD, USA) were performed as described (User's manual from Origene Technologies Inc.). For screening the cDNA library, the bait vector pEG202-$D2^{3rd}$ was transformed into yeast strain EGY48 using a lithium acetate protocol after transforming EGY48 with a LacZ reporter plasmid, pSH18–34. Transformation of EGY48 with both LacZ reporter plasmid and the bait plasmid confirmed that there was no interaction between LexA-D_2^{3rd} and reporter operator for inducing the expression of LacZ, indicating no blue color on X-Gal media lacking histidine and uracil (β-galactosidase assay). Also, there was no induction of leucine in EGY48 with bait plasmid, showing no growth on media lacking histidine, uracil, and leucine. The EGY48 strains harboring the reporter plasmids and the bait plasmids were transformed with the rat cDNA brain library and the transformants expressing the bait and interacting prey proteins were selected on medium lacking histidine, uracil, and tryptophan. The positive clones (His+, Ura+, and Trp+) were selected for further characterization. Plasmids from the selected clones were isolated using the yeast DNA isolation system and amplified in *Escherichia coli*. DNA sequencing was performed by the NINDS sequencing facility (Bethesda, MD, USA) using automated methods.

Cell culture and transfections

Human embryonic kidney (HEK293T) cells were cultured in Dulbecco's modified Eagle's medium (DMEM) supplemented with 10% fetal calf serum, 50 U/mL penicillin, 50 μg/mL streptomycin, and 10 μg/mL gentamycin. Cells were grown at 37°C in 5% CO_2 and 90% humidity. Expression vectors used to transfect HEK293T cells were as follows: D_2 DAR FLAG, ZIP1-Myc, ZIP3-Myc (gifts of Dr R. Enz), ZIP1-HA, and ZIP2-HA (gifts of Dr M. Li). For transfection, the calcium–phosphate precipitation method was used. Cells were seeded in 150- or 100-mm^2 plates and transfection was carried out when cells were ~50% confluent. DNA and 60 or 36 μL of 2 M $CaCl_2$ were mixed in H_2O in a total volume of 500 or 300 μL and then slowly mixed with HEPES-buffered saline. The reaction mixture was incubated at 22°C for 25 min and then evenly added to the cell culture dish containing 20 or 10 mL of fresh media. After 16–18 h, the transfection media was replaced with fresh media and the cells were harvested the following day for the assays.

Immunoprecipitation and western blot analyses

Approximately 48 h after transfection, HEK293T cells were washed twice with ice-cold phosphate-buffered saline (PBS) and solubilized for 1 h at 4°C in 500 μL of solubilization buffer (50 mM HEPES, 1 mM EDTA, 10% glycerol, and 1% Triton X-100, pH 7.4 at 4°C) +150 mM NaCl supplemented with complete protease inhibitor cocktail and phosphatase inhibitors (40 μM sodium pyrophosphate and 50 μM NaF). The supernatants were collected by centrifugation for 30 min at 13 000 *g* and the protein concentration was determined by the BCA assay. The same amount of protein in each sample (~400 μg) was incubated with 25 μL Ezview red anti-FLAG affinity agarose in solubilization buffer overnight at 4°C with an end–end rotation. After centrifugation, the agarose gels were washed with solubilization buffer plus 150 mM NaCl, lysis buffer plus 500 mM NaCl, and with Tris–EDTA (TE, pH 7.4) sequentially to remove non-specific bound proteins. The agarose gels were incubated in 2× sodium dodecyl sulfate (SDS) sample loading buffer for 1 h at 37°C and the proteins were resolved by SDS–polyacrylamide gel electrophoresis (PAGE). The separated proteins were transferred to polyvinylidene difluoride (PVDF) membrane. The PVDF membrane was incubated with anti-Myc antisera conjugated with HRP, anti-HA-HRP, or anti-FLAG-HRP (1 : 5000) for 1 h at 22°C after incubated in Tris-buffered saline and 0.1% Tween 20 containing 5% non-fat milk for 1 h at 22°C. The PVDF membrane was washed four times for 5 min each and developed using with Super signal DURA or PICO chemiluminescent substrate.

For immunoprecipitation (IP) of brain tissues, the brains of wild-type and D_2 DAR knockout mice were homogenized in lysis buffer using a glass–glass homogenizer, sonicated for 1 min, and incubated on ice for 1 h. The supernatants were saved after centrifugation of the homogenized brain tissues for 30 min at 13 000 *g*. The supernatant was incubated with Ezview red protein G affinity gel to remove proteins that bound to the gel non-specifically for 3 h. The supernatants were incubated with anti-ZIP antibodies overnight at 4°C and incubated with Ezview red protein G affinity gel for 1 h. Proteins bound to ZIP-affinity gel were washed with lysis buffer three times and boiled in SDS sample buffer for 10 min. The proteins were separated by 10% SDS–PAGE and transferred onto PVDF membrane. Western blot analysis was carried out with anti-D_2 DAR antibodies.

Immunohistochemistry and fluorescence microscopy

Fresh frozen rat brains were sectioned at 10 μm and mounted onto slides. Sections were fixed for 5 min in freshly prepared 4% *p*-formaldehyde in PBS (4°C). After a 5 min rinse in PBS, sections were incubated simultaneously with both primary antisera overnight in a moist environment (4°C). Rabbit-derived D_2 DAR antisera have been well characterized (McVittie *et al.* 1991) and were applied at 1 : 200 dilution in PBS. ZIP antisera were raised in goats (sc-8161 and sc-8162) and diluted 1 : 200 in PBS. Primary antisera were rinsed off with PBS the following day; secondary reagents were diluted 1 : 200 in PBS, applied together as Cy2 and Cy3 conjugates and incubated 2 h at (4°C) in a moist environment. Sections were given a final PBS rinse and examined immediately using fluorescence microscopy. Brain sections processed for immunohistochemistry were examined using standard epifluorescence microscopy (Olympus BX41, Optical Analysis Co., Nashua, NH, USA). Digitized images of the experimental tissues in different brain areas were made with a megapixel camera (Optronics, Goleta, CA, USA). Image acquisition parameters for each antisera staining experiment were optimized to use the entire gray scale range (0–255). At least four different experimental incubations were evaluated for the combined D_2 DAR and ZIP staining. The fluorescent staining reactions were stored and electronically merged using Adobe Photoshop™ off-line (Adobe Systems, Mountain View, CA, USA).

Radioligand-binding assays

Cells were harvested by incubation with 5 mM EDTA in Dulbecco’s phosphate-buffered salt solution and collected by centrifugation at 300 *g* for 10 min. The cells were re-suspended in lysis buffer (5 mM Tris, pH 7.4 at 4°C, and 5 mM $MgCl_2$) and were disrupted using a dounce homogenizer followed by centrifugation at 35 000 g for 20 min. The resulting membrane protein pellet was re-suspended in binding buffer (50 mM Tris, pH 7.4). The membrane suspension (final protein concentration 20–30 μg/tube) was then added to assay tubes containing [^{3}H]methylspiperone (for D_2 DAR) or [^{3}H]SCH 23390 (for D_5 DAR) in a final volume of 1.0 mL. (+)-Butaclamol was added at the final concentration of 3 μM to determine non-specific binding. The assay tubes were incubated at 22°C for 1.5 h and the reaction was terminated by rapid filtration through GF/C filters (Brandel, Gaithersburg, MD, USA) pre-treated with 0.3% polyethyleneimine. Radioactivity bound to the filters was quantitated by liquid scintillation spectroscopy at a counting efficiency of 57%. Radioligand-binding assays were routinely performed in triplicate and were repeated three to nine times. Estimation of the radioligand-binding parameters, K_d and B_{max}, were calculated using the GraphPad Prism curve-fitting program (GraphPad Software Inc., San Diego, CA, USA).

Determination of cAMP production

Cyclic AMP was quantified using a competitive-binding assay adapted from the method of Watts and Neve (1996) with modifications. HEK293 cells were seeded into poly-D-lysine coated 24-well plates 1 day after transfection at a density of 2 × 10 cells per well. The cells were washed once with pre-warmed Earle's balanced salt solution (EBSS) and then incubated with various concentrations of DA in a total volume of 0.4 mL at 37°C for 10 min in the presence of 3 μM forskolin, 30 μM Ro-20–1724 (phosphodiesterase inhibitor), 0.2 mM sodium metabisulfite (to prevent oxidation of DA), and 10 μM propranolol (to block endogenous β-adrenergic receptors) in 20 mM HEPES-buffered DMEM. The supernatant was aspirated, and perchloric acid (3%, 200 μL/well) was added. After incubating on ice for 30 min, 80 μL of 15% KHCO3 was added to the wells and the plates were further incubated for 10 min. The plates were then centrifuged for 10 min at 1300 *g*; 50 mL of the supernatant from each well was subsequently transferred to a 1.2 mL tube containing 150 μL TE buffer (100 μM Tris and 5 mM EDTA, pH 7.4); 50 μL of [^{3}H]cAMP (~6 nM, final ~1 nM concentration) was added to each tube, followed by 50 μL of cAMP-binding protein. After incubation at 4°C for 3 h, 250 μL of pre-chilled charcoal suspension (2% carbon and 0.5% bovine serum albumin) was added each tube followed by incubation at 4°C for 15 min then centrifugation for 15 min at 1300 *g*. Radioactivity in the supernatant from each tube was quantified by liquid scintillation spectroscopy. cAMP concentrations were estimated in duplicate from a standard curve ranging from 0.1 to 27 pmol of cAMP/assay.

Whole cell phosphorylation assays

Metabolic labeling of cells and subsequent IP of the D_2 DAR was carried out as described previously (Gardner *et al.* 2001). Briefly, HEK293T cells were transfected with D_{2L} DAR FLAG using calcium–phosphate method. One day after transfection, cells were seeded at 1–1.5 × 10^6 per well of a poly-D-lysine coated six-well plate for phosphorylation assay and ~2 × 10^6 cells on 100 mm dish for radioligand-binding assay to quantify the level of receptor expression. The next day, the cells were washed with EBSS and incubated for 1 h in phosphate-free DMEM with 10% fetal calf serum. Media was removed and replaced with 1 mL of fresh media supplemented with 200 μCi/mL [^{32}P]H_3PO_4. After 45 min at 37°C, the cells were then challenged with 100 nM insulin or 1 μM phorbol-12-myristate-13-acetate. Cells were then transferred to ice, washed twice with ice-cold EBSS, and solubilized for 1 h at 4°C in 1 mL of solubilization buffer. The samples were cleared by centrifugation in a microfuge at 10 000 *g* and the protein concentration was determined by BCA assay. The level of D_2 DAR expression for each transfection was quantified via radioligand-binding assays using the cells from the same transfection. After receptor/protein quantification, equal amounts of receptor protein were then transferred to fresh tubes with 40 μL of washed anti-M2-agarose and incubated overnight with mixing at 4°C. The samples were then washed once with solubilization buffer and 500 mM NaCl, once with solubilization buffer and 150 mM NaCl, and once with TE, pH 7.4 at 4°C. Samples were then incubated in 2× SDS–

PAGE loading buffer for 1 h at 37°C before being resolved by 4– 20% Tris–glycine SDS–PAGE. The gels were dried and subjected to autoradiography. After developing, the band intensity was quantitated by LabWorks™ software (UVP Inc., Upland, CA, USA).

Confocal microscopy

A total of 300 000 HEK293T cells were seeded in 100 mm culture dishes. The next day, the cells were transfected with 100 ng of D_2 DAR-yellow fluorescent protein (YFP) and 1.0 mg of either pcDNA (control) or ZIP1, then cultured for an additional 24 h prior to reseeding the transfection at 100 000 cells per poly-D-lysine-coated, glass-bottom 35 mm culture dish. On the day of the experiment, the cells were incubated with or without 75 μM LysoTracker Red for 90 min prior to imaging using confocal microscopy on a Zeiss laser-scanning confocal microscope (LSM-510, Thornwood, NY, USA). Images were collected using a single line excitation (488 nm).

Results

Identification of ZIP1 as an interacting protein of the D_2 DAR

To identify proteins that interact with the D_2 DAR, we performed a Y2H screen using the IC3 (amino acids Lys211– Gln374) of the D_{2L} DAR protein as bait (Fig. 1). Screening of a rat whole brain cDNA library yielded several potential interacting partners and one clone, s330, encoding a fragment of ZIP1 (Puls *et al.* 1997) was selected for further characterization. Complete sequencing of clone s330 revealed that it contained amino acids, K184 to E378 of ZIP1 (Fig. 2a). The full-length ZIP1 protein is 439 residues in length and contains a number of protein interaction domains (Fig. 2b) (Puls *et al.* 1997; Wooten *et al.* 2001). To evaluate the specificity of the D_2 DAR–ZIP interaction, we examined the interaction of the partial-length ZIP1 clone with the third cytoplasmic domains of all DAR subtypes (Table 1). No interaction was detected with D_3 or D_4 DARs of the D_2 subfamily or with members of the D_1 subfamily of DARs, D1 or D_5 (Table 1). These results suggested that the interaction between the D_2 DAR and the ZIP1 clone, s330, is specific in nature.

Mapping the D_2 DAR–ZIP1 interaction domain

To further map the ZIP1 interaction domain within the IC3 of the D_2 DAR, we generated truncation mutants, T0, T1, and T2, of the D_2^{3rd} loop as shown in Fig. 1. T0 encodes third loop residues Lys211–Leu240, T1 encodes residues Lys211– Asp271, and T2 encodes residues Lys211–Ser311. These constructs were evaluated for their ability to interact with the ZIP1 clone using the Y2H assay. Yeast cells transformed with either D_2 DAR-T1 or D_2 DAR-T2 and ZIP1 were able to grow in the absence of leucine, histidine, uracil, and tryptophan and were also able to activate the reporter gene LacZ using X-Gal as the substrate (Table 1). However, yeast cells transformed with D_2 DAR-T0 and ZIP1 were not able to grow or activate LacZ (Table 1). These results appear to narrow the ZIP1-binding domain in the D_2^{3rd} loop to within Lys241–Asp271 of D_2 DAR. The amino acid residues from Gly242 to Met270, indicated as black circles in Fig. 1, are absent in the shorter RNA splice variant of the D_2 receptor (D_{2S}) (Bunzow *et al.* 1988; Giros *et al.* 1989; Monsma *et al.* 1989). Interestingly, using the Y2H assay, we found that the D_{2S} IC3 also interacted with the ZIP1 clone (data not shown). Thus, these results suggest that either Lys241 and/or Asp271 within the IC3 of the D_2 DAR are required for interaction with ZIP1. Future mutagenesis studies should shed light on this issue.

D_2 DAR binds to ZIP1 in mammalian cells

To verify whether the full-length D_2 DAR and full-length ZIP1 proteins interact in mammalian cells, HEK293T were transiently transfected with the expression constructs, D_2-FLAG and/or ZIP1-Myc (Croci *et al.* 2003). At 48 h post-transfection, lysates from cells transfected with empty vector (pcDNA), D_2-FLAG, ZIP1-Myc, or both D_2-FLAG and ZIP1-Myc were immunoprecipitated with anti-FLAG antibodies, electrophoresed, and blotted with anti-Myc antibodies. As shown in Fig. 3a (lane 4), ZIP1 co-immunoprecipitated with the D_2 DAR. ZIP1-Myc was detected only from cells transfected with both D_2-FLAG and ZIP1-Myc, but not in cells transfected with either construct alone (lanes 2 and 3 in Fig. 3a). These results provide biochemical confirmation that the D_2 DAR and ZIP1 are capable of directly interacting in mammalian cells.

We were also interested in establishing that the D_2 DAR interacts with ZIP1 in native neuronal tissues. Consequently, we performed co-IP experiments using brain tissue from wild-type mice as well as D_2 DAR knockout mice (Kelly *et al.* 1997). Figure 3b shows that when ZIP1 is immunoprecipitated from whole brain lysates, and the resulting protein complexes electrophoresed followed by probing with an anti-D_2 DAR antibody, four protein species of ~250, 100, 75, and 55 kDa were observed in brains from wild-type, but not D_2 DAR-deficient mice. These proteins may correspond to various glycosylation and/or oligomeric forms of the D_2 DAR (Worsley *et al.* 2000; Kameda *et al.* 2001). The absence of these protein species in the D_2 DAR knockout brain tissue further establishes their specificity. The ability of ZIP1 to co-immunoprecipitate the D_2 DAR from brain tissue thus confirms that ZIP1 and the D_2 DAR directly interact in the brain.

D_2 DAR and ZIP1 are co-localized in brain tissue

To establish that the D_2 DAR and ZIP1 are co-localized in specific brain regions, we performed immunohistochemical analyses of rat striatum and cortex. Immunofluorescent detection of ZIP1 (green label) and D_2 DAR (red label) was performed using fresh-frozen rat brain sections (Fig. 4). The striatum (Fig. 4a) shows numerous medium-sized neuronal somata that co-express the D_2 DAR and ZIP1 and are apparent as yellow signals. ZIP1 exhibits strong reactions within the neuropil, but both proteins are absent from the fiber bundles of the internal capsule. Figure 4b shows that neurons within layers 3–6 of the somatosensory cortex also co-stained for ZIP1 and D_2 DAR (yellow signals, filled arrow). Occasional neurons were only reactive for D_2 DAR (red signal, arrow), while a few neurons showed only ZIP staining (green signal, open arrow). Figure 4c shows a higher magnification of the cortex clearly demonstrating the coincidence of the two antigens. ZIP1-reactive processes are visible emanating from the somata, and show heterogeneous, punctate distributions throughout the neuropil. Taken together, these results show that the D_2 DAR and ZIP1 are extensively co-localized at the cellular level within specific regions of the brain.

D_2 DAR interacts with all three RNA splice variants of ZIP

Protein kinase C-ζ interacting protein 1 RNA can be alternatively spliced to yield two shorter versions of ZIP1, ZIP2, and ZIP3 (Fig. 5a) (Gong *et al.* 1999; Croci *et al.* 2003). To determine whether the D_2 DAR interacts with the other two RNA splice variants of ZIP1, we co-expressed D_2 DAR-FLAG with either ZIP2-HA or ZIP3-Myc in HEK293T cells. Forty-eight hours after transfection, cells were harvested and whole cell lysates were incubated with anti-FLAG antibodies to immunoprecipitate the D_2 DAR. Following electrophoresis anti-Myc antibodies was used to detect ZIP3 and anti-HA antibodies to detect ZIP1 and ZIP2. All three splice variants, the proteins ZIP1, ZIP2, and ZIP3 were co-immunoprecipitated with the D_2 DAR as shown in lanes 2, 3, and 4 of Fig. 5b. These results indicate that all three RNA splice variants of ZIP are capable of interacting with the D_2 DAR. In addition, these results, together with the partial-length ZIP cDNA sequence, further suggest that the binding domain of ZIP to D_2 DAR is between Lys184 and Ser221 (hatched box in Figs 2a and 5a) as residues Ala222 to Lys248 and Ser223 to Lys439 are absent in ZIP2 and ZIP3, respectively (Fig. 5a). However, ZIP3 has an additional 13 amino acids right after Ala222 (Fig. 5a) (Croci *et al.* 2003).

D_2 DAR expression is reduced by over-expression of ZIP1

To investigate functional interactions between ZIP1 and the D_2 DAR, we initially expressed both proteins in HEK293T cells and examined receptor expression levels using radioligand-binding assays in membrane preparations (Fig. 6). With over-expression of ZIP1, the maximum membrane-binding capacity of the D_2 DAR was reduced by over 50% compared with control cells which were co-transfected with empty vector instead of ZIP1 (Fig. 6a). This reduction in binding capacity appears to be because of a decrease in total receptor number (B_{max}) rather than a change in affinity (K_d) for the radioligand. As equal amounts of DNA were used in each transfection group, the decreased expression of the D_2 DAR appears to be a direct result of ZIP1 over-expression rather than a decreased efficiency of transfection for the D_2 DAR construct. In contrast to the reduction in D_2 DAR expression, there was no effect of co-expressing full-length ZIP1 on the expression of the D_1-like DARs D_5 (Fig. 6b) or D_1 (data not shown).

Interestingly, we found that the expression of the other D_2-like DAR subfamily members, D_3 and D_4, was also reduced in a manner similar to that of D_2 DAR when ZIP1 was co-expressed (data not shown). There are several possible explanations for this finding despite the negative Y2H assay results examining interactions between the D_3 and D_4 third loops and the partial-length ZIP1 clone (Table 1). First, it is conceivable that ZIP1 interacts with the D_3 and D_4 DARs through other receptor domains outside of the IC3. Similarly, it is also possible that the D_3 and D_4 DARs interact with ZIP1 domains outside those present in the partial-length s330 clone. Finally, the interactions of the D_3 and D_4 DARs IC3 with ZIP1 may be more dependent on conformations imparted within the holo-receptors compared with that of the D_2 DAR, thus explaining the negative Y2H results. While this remains to be determined and further characterized, it appears as if ZIP1 is capable of modifying the expression of all D_2 DAR subfamily members.

ZIP1 attenuates D_2 DAR signaling in HEK293 cells

We were next interested in examining for potential effects of ZIP1 on D_2 DAR function via cAMP-mediated signaling. In D_2 DAR-transfected cells, DA dose-dependently inhibits forskolin-stimulated cAMP accumulation (Fig. 7). In the control cell group, the maximum inhibition of cAMP accumulation by DA is about 80% with an EC_{50} of 12.4 nM. Over-expression of ZIP1 in these cells results in an attenuation of D_2 DAR-mediated inhibition of cAMP accumulation (Fig. 7). In this case, DA promotes only a ~40% inhibition of cAMP accumulation and the EC50 for this response is shifted approximately sixfold to lower potency. Taken together, the results in Figs 6 and 7 clearly indicate that ZIP1 negatively modulates D_2 DAR expression and functional signaling.

ZIP1 promotes D_2 receptor trafficking to lysosomes in HEK293T cells

As ZIP1 over-expression was found to reduce D_2 DAR expression, we were next interested in determining if ZIP1 might alter intracellular trafficking of the receptor. As D_2 DARs appear to be trafficked to, and degraded within lysosomes upon internalization (Kallal *et al.* 1998; Moore *et al.* 1999; Whistler *et al.* 2001; Liang *et al.* 2004), we examined co-localization of the DARs with lysosomes via confocal fluorescent microscopy. Figure 8a shows HEK293T cells that have been treated with LysoTracker Red, a dye that specifically accumulates in the acidic organelles such as lysosomes which are clearly visualized. Figure 8b shows HEK293T cells transfected with a fusion protein of the D_2 DAR and YFP. As can be seen, most of the D_2 DAR fluorescence is present at the cell surface, although some receptor is also localized intracellularly in vesicle-like compartments. Figure 8c shows D_2-YFP expressing cells that have been treated with LysoTracker Red. Notably, as indicated by the yellow vesicular staining, some of the intracellular D_2 receptor is localized within lysosomal compartments. Figure 8d shows HEK293T cells that have been co-transfected with D_2-YFP and ZIP1. In contrast to that observed in Fig. 8b/c, there much less expression of the D_2 receptor at cell surface with a corresponding increase in receptor located within intracellular vesicular compartments. Finally, Fig. 8e shows cells co-transfected with D_2-YFP and ZIP1 and treated with LysoTracker Red. In this case, the majority of the intracellular D_2 DARs appear to be co-localized within lysosomes. These results suggest that over-expression of ZIP1 results in increased trafficking of internalized D_2 DARs to lysosomes, which likely leads to their subsequent degradation and down-regulation.

ZIP1 does not promote PKCζ-mediated phosphorylation of the D_2 DAR

As we have previously shown that the D_2 DAR undergoes PKC-mediated phosphorylation, which in turn promotes receptor internalization (Namkung and Sibley 2004), we wondered if ZIP1 might also promote PKCζ-mediated D_2 DAR phosphorylation. To investigate this, we co-expressed the D_2 DAR with or without ZIP1 and/or PKCζ and examined the phosphorylation state of the DAR. Figure 9a shows that the D_2 DAR is phosphorylated in the basal state as we have previously described (Namkung and Sibley 2004). Treatment of the cells with insulin, which is known to lead to PKCζ activation, has no effect on the phosphorylation state of the D_2 DAR (left two lanes). Over-expression of ZIP1 has no effect, although insulin treatment leads to enhanced ZIP1 phosphorylation evident as the ~62 kDa protein in the gel (Fig. 9a, middle two lanes). This agrees with the observation that PKCζ can phosphorylate ZIP using *in vitro* kinase assays (Puls *et al.* 1997). Similarly, over-expression of ZIP1 and PKCζ has no effect on D_2 DAR phosphorylation (Fig. 9a, right two lanes) although ZIP1 phosphorylation appears to be slightly reduced. As a control, we over-expressed PKCβ with the D_2 DAR, which clearly leads to increased basal, as well as phorbol-12-myristate-13-acetate ester-stimulated receptor phosphorylation (Fig. 9b). These results indicate that PKCζ, or receptor phosphorylation, is not involved in mediating ZIP1s effects on D_2 DAR expression and function.

Discussion

Recent studies have emerged that DARs interact with other molecules, ion channels, and receptors to form macromolecular signaling complexes, which mediate the activities of the neurotransmitter DA and its congeners (Binda *et al.* 2002; Kabbani and Levenson 2007; Kim *et al.* 2002; Bergson *et al.* 2003; Jeanneteau *et al.* 2004; Park *et al.* 2005; Free *et al.* 2007). Most of the identified DRIPs bind to the second cytoplasmic loop, the IC3, or the C-terminal tail of the DARs. Although all the functions of these DRIPs have not been completely elucidated, DRIPs appear to be involved in regulating signaling, scaffolding, trafficking, or localization of DARs in the plasma membrane (Binda *et al.* 2002; Kabbani *et al.* 2002; Kim *et al.* 2002; Bergson *et al.* 2003; Park *et al.* 2005; Free *et al.* 2007).

In this report, we identified PKCζ interacting protein, ZIP1 as a novel DRIP of the rat D_2 DAR (Puls *et al.* 1997). No interaction was observed between ZIP1 and the IC3 of the D_1 subfamily of DARs (D_1 and D_5) as well as with the D_3 and D_4 DARs of the D_2 subfamily of DARs, although D_3 and D_4 DAR expression was reduced by over-expression of ZIP. The IC3 of the D_2 DAR is known to couple to G proteins and to interact with other molecular elements involved in DA-mediated synaptic neurotransmission. ZIPs interaction with the D_2 DARs IC3 reduced receptor expression at the cell surface and also reduced the potency and maximum response for DA-promoted inhibition of cAMP accumulation. While it might be expected that the ZIP-induced reduction in receptor expression would reduce the maximum functional response by DA, the reduction in agonist potency as well suggests the possibility that ZIP interaction with the D_2 DARs IC3 may additionally impair receptor-G protein coupling.

To map the ZIP1-binding domain within the D_2 DAR IC3, we generated several truncation mutants, which were evaluated using the Y2H assays. This, along with assays including the D_2S IC3 loop, lead to the conclusion that two amino acids adjacent to the D_2S DAR splice site, K241 and D271 might be critical for the interactions of the D_2 DAR with ZIP. We thus speculate from these results that one or both of these amino acids are involved in the formation of the ZIP-D_2 DAR complex. Further work involving site-directed mutagenesis of these residues will address this issue more directly.

Protein kinase C-ζ interacting protein 1 is the longest isoform of ZIP family which includes the splice variants, ZIP1, ZIP2, and ZIP3 (Puls *et al.* 1997; Gong *et al.* 1999; Croci *et al.* 2003). The D_2 DAR interacts with all three ZIP isoforms indicating that the binding domain of ZIP1 to D_2 DAR is within the 38 amino acids upstream of the splice site of ZIP (see Fig. 5a). Interestingly, this domain contains one of the three putative PKC-binding sites of ZIP1 suggesting that a ternary complex of PKCζ/ZIP1/D_2 DAR may not be possible, although the formation of PKCζ/ZIP1/Kvβ2 and PKCζ/ZIP3/$GABA_C$ complexes have been demonstrated (Gong *et al.* 1999; Croci *et al.* 2003). When ZIP1 and ZIP2 were expressed together, they acted synergistically in promoting PKCζ to phosphorylate the Kvβ2 subunit (Gong *et al.* 1999). In contrast, we found that the D_2 DAR was not phosphorylated by PKCζ when ZIP1 was co-expressed. These results further suggest that a ternary complex of PKCζ/ZIP1/D_2DAR may not exist and that the linkage of the D_2 DAR to ZIP1 is not regulated by PKCζ-mediated phosphorylation.

Protein kinase C-ζ interacting protein 1 is highly homologous to p62, an apparent human homolog, and also to A170, a mouse homolog (Ishii *et al.* 1996; Joung *et al.* 1996; Puls *et al.* 1997). The structural motifs shared by these three proteins include an Src homology 2 binding domain, an acidic interaction domain that binds the atypical PKC, a zinc finger binding site, a binding site for the ring-finger protein, tumor necrosis factor receptor-associated factor 6, two PEST (Pro-Glu-Ser-Thr) sequences, and a ubiquitin-associated domain (Joung *et al.* 1996; Puls *et al.* 1997; Gong *et al.* 1999; Wooten *et al.* 2001; Croci *et al.* 2003). The high degree of sequence similarity between these proteins suggests conserved functionality. ZIP1 is also suggested to have affinity for ubiquitin as the C-terminal domain of p62 is completely conserved in both ZIP1 and A170, and p62 is capable of binding ubiquitin non-covalently (Vadlamudi *et al.* 1996; Seibenhener *et al.* 2004). A170/ZIP1/p62 has also been identified as a 'sequestosome' as A170/ZIP1/p62 preferentially binds multiubiquitin chains and forms a cytoplasmic structure which serves as a storage for ubiquitinated proteins (Shin 1998).

The co-IP of D_2 DAR and ZIP1 from HEK293T cells and from mouse brain tissue suggests a functional relationship *in vivo*. To further investigate potential interactions *in vivo*, immunohistochemical analyses were performed which showed that the D_2 DAR and ZIP1 were co-expressed in neurons within the striatum and the cortex of adult rat brain, suggesting that the ZIP1 can interact with the D_2 DAR in normal brain. The interaction of D_2 DAR and ZIP in brain tissue is intriguing based on recent findings from other laboratories (Nakaso *et al.* 1999, 2004; Kuusisto *et al.* 2001, 2002; McNaught and Jenner 2001; Zatloukal *et al.* 2002) showing the ubiquitin-proteasome system is one of the pathways involved in detoxification and degradation of damaged proteins during neurodegeneration (Ciechanover and Brundin 2003). Interestingly, p62 appears to be a common component of cytoplasmic inclusion bodies (Zatloukal *et al.* 2002) such as Lewy bodies in Parkinson's disease (Kuusisto *et al.* 2001) and in neurofibrillary tangles in Alzheimer's disease (Vadlamudi *et al.* 1996; Kuusisto *et al.* 2001). These observations suggest that ZIP1/p62/A170 may play a role in the pathogenesis of these diseases through the formation of inclusion bodies. ZIP1/p62/A170 is also expressed at high levels in neuronal cells in the brain and its expression level is up-regulated at the transcriptional level in pyramidal neurons or Purkinje cells by kainite-mediated excitotoxicity (Nakaso *et al.* 1999). ZIP1/p62/A170 also plays a significant role in nerve growth factor-related signal transduction during the differentiation of neuronal cells (Wooten *et al.* 2001). Therefore, the interaction of D_2 DAR with ZIP1 in brain tissue may play an important role in neuronal pathogenesis.

In summary, we have identified ZIP as a novel interacting protein of the D_2 DAR. We show that the association of ZIP and the D_2 DAR is functional where over-expression of ZIP reduces the cell surface expression of the receptor and inhibits its ability to reduce cAMP accumulation. ZIP1 also promotes trafficking of the D_2 DAR to lysosomes where the receptors are subsequently degraded (Kallal *et al.* 1998; Moore *et al.* 1999; Whistler *et al.* 2001). Our finding that the expression and function of the D_2 DAR is regulated by ZIP, the expression of which is inducible by oxidative stress (Ishii *et al.* 1996; Wang *et al.* 2007) may also provide a novel mechanism by which the D_2 DAR is regulated under conditions of oxidative stress.

Acknowledgments

The authors would like to thank to Dr Min Li for ZIP1-HA and ZIP2-HA constructs, to Dr Ralf Enz for ZIP1-myc and ZIP3-myc constructs. This research was supported by the Intramural Research Program of NINDS, NIH to DRS and by the University of Kansas General Research Fund allocation #2301813 to O-JK.

Abbreviations used

BCA	bicinchoninic acid protein
DA	dopamine
DAR	dopamine receptor
DMEM	Dulbecco's modified Eagle's medium
DRIP	dopamine receptor interacting protein
EBSS	Earle's balanced salt solution
HA	hemagglutinin
HEK	human embryonic kidney cells
HRP	horseradish peroxidase
IC3	third cytoplasmic loop
IP	immunoprecipitation
PAGE	polyacrylamide gel electrophoresis
PBS	phosphate-buffered saline
PKC	protein kinase C
PKC	protein kinase C
PVDF	polyvinylidene difluoride
SDS	sodium dodecyl sulfate
TE	Tris–EDTA

Y2H	yeast two-hybrid
YFP	yellow fluorescent protein
ZIP	protein kinase C-ζ interacting protein

References

Bergson C, Levenson R, Goldman-Rakic PS, Lidow MS. Dopamine receptor-interacting proteins: the Ca(2+) connection in dopamine signaling. Trends Pharmacol. Sci. 2003; 24:486–492. [PubMed: 12967774]

Binda AV, Kabbani N, Lin R, Levenson R. D2 and D3 dopamine receptor cell surface localization mediated by interaction with protein 4.1N. Mol. Pharmacol. 2002; 62:507–513. [PubMed: 12181426]

Bunzow JR, Van Tol HH, Grandy DK, Albert P, Salon J, Christie M, Machida CA, Neve KA, Civelli O. Cloning and expression of a rat D2 dopamine receptor cDNA. Nature. 1988; 336:783–787. [PubMed: 2974511]

Ciechanover A, Brundin P. The ubiquitin proteasome system in neurodegenerative diseases: sometimes the chicken, sometimes the egg. Neuron. 2003; 40:427–446. [PubMed: 14556719]

Croci C, Brandstatter JH, Enz R. ZIP3, a new splice variant of the PKC-zeta-interacting protein family, binds to GABAC receptors, PKC-zeta, and Kv beta 2. J. Biol. Chem. 2003; 278:6128–6135. [PubMed: 12431995]

Free RB, Hazelwood LA, Cabrera DM, Spalding HN, Namkung Y, Rankin ML, Sibley DR. D1 and D2 dopamine receptor expression is regulated by direct interaction with the chaperone protein calnexin. J. Biol. Chem. 2007; 282:21285–21300. [PubMed: 17395585]

Gardner B, Liu ZF, Jiang D, Sibley DR. The role of phosphorylation/dephosphorylation in agonist-induced desensitization of D1 dopamine receptor function: evidence fora novel pathway for receptor dephosphorylation. Mol. Pharmacol. 2001; 59:310–321. [PubMed: 11160868]

Giros B, Sokoloff P, Martres MP, Riou JF, Emorine LJ, Schwartz JC. Alternative splicing directs the expression of two D2 dopamine receptor isoforms. Nature. 1989; 342:923–926. [PubMed: 2531847]

Gong J, Xu J, Bezanilla M, van Huizen R, Derin R, Li M. Differential stimulation of PKC phosphorylation of potassium channels by ZIP1 and ZIP2. Science. 1999; 285:1565–1569. [PubMed: 10477520]

Ishii T, Yanagawa T, Kawane T, Yuki K, Seita J, Yoshida H, Bannai S. Murine peritoneal macrophages induce a novel 60-kDa protein with structural similarity to a tyrosine kinase p56lck-associated protein in response to oxidative stress. Biochem. Biophys. Res. Commun. 1996; 226:456–460. [PubMed: 8806656]

Jeanneteau F, Diaz J, Sokoloff P, Griffon N. Interactions of GIPC with dopamine D2, D3 but not D4 receptors define a novel mode of regulation of G protein-coupled receptors. Mol. Biol. Cell. 2004; 15:696–705. [PubMed: 14617818]

Joung I, Strominger JL, Shin J. Molecular cloning of a phosphotyrosine-independent ligand of the p56lck SH2 domain. Proc. Natl Acad. Sci. USA. 1996; 93:5991–5995. [PubMed: 8650207]

Kabbani N, Levenson R. A proteomic approach to receptor signaling: molecular mechanisms and therapeutic implications derived from discovery of the dopamine D(2) receptor signalplex. Eur. J. Pharmacol. 2007; 57:83–93.

Kabbani N, Negyessy L, Lin R, Goldman-Rakic P, Levenson R. Interaction with neuronal calcium sensor NCS-1 mediates desensitization of the D2 dopamine receptor. J. Neurosci. 2002; 22:8476–8486. [PubMed: 12351722]

Kallal L, Gagnon AW, Penn RB, Benovic JL. Visualization of agonist-induced sequestration and down-regulation of a green fluorescent protein-tagged beta2-adrenergic receptor. J. Biol. Chem. 1998; 273:322–328. [PubMed: 9417083]

Kameda K, Miura J, Suzuki K, Kusumi I, Tanaka T, Koyama T. Effects of lithium on dopamine D2 receptor expression in the rat brain striatum. J. Neural Transm. 2001; 108:321–334. [PubMed: 11341484]

Kelly MA, Rubinstein M, Asa SL, et al. Pituitary lactotroph hyperplasia and chronic hyperprolactinemia in dopamine D2 receptor-deficient mice. Neuron. 1997; 19:103–113. [PubMed: 9247267]

Kim OJ, Ariano MA, Lazzarini RA, Levine MS, Sibley DR. Neurofilament-M interacts with the D1 dopamine receptor to regulate cell surface expression and desensitization. J. Neurosci. 2002; 22:5920–5930. [PubMed: 12122054]

Kuusisto E, Salminen A, Alafuzoff I. Ubiquitin-binding protein p62 is present in neuronal and glial inclusions in human tauopathies and synucleinopathies. Neuroreport. 2001; 12:2085–2090. [PubMed: 11447312]

Kuusisto E, Salminen A, Alafuzoff I. Early accumulation of p62 in neurofibrillary tangles in Alzheimer's disease: possible role in tangle formation. Neuropathol. Appl. Neurobiol. 2002; 28:228–237.

Liang W, Curran PK, Hoang Q, Moreland RT, Fishman PH. Differences in endosomal targeting of human (beta)1- and (beta)2-adrenergic receptors following clathrin-mediated endocytosis. J. Cell Sci. 2004; 117:723–734. [PubMed: 14734649]

McNaught KS, Jenner P. Proteasomal function is impaired in substantia nigra in Parkinson's disease. Neurosci. Lett. 2001; 297:191–194. [PubMed: 11137760]

McVittie LD, Ariano MA, Sibley DR. Characterization of anti-peptide antibodies for the localization of D2 dopamine receptors in rat striatum. Proc. Natl Acad. Sci. USA. 1991; 88:1441–1445. [PubMed: 1825357]

Missale C, Nash SR, Robinson SW, Jaber M, Caron MG. Dopamine receptors: from structure to function. Physiol. Rev. 1998; 78:189–225. [PubMed: 9457173]

Monsma FJ, McVittie LD Jr, Gerfen CR, Mahan LC, Sibley DR. Multiple D2 dopamine receptors produced by alternative RNA splicing. Nature. 1989; 342:926–929. [PubMed: 2480527]

Moore RH, Tuffaha A, Millman EE, Dai W, Hall HS, Dickey BF, Knoll BJ. Agonist-induced sorting of human beta2-adrenergic receptors to lysosomes during downregulation. J. Cell Sci. 1999; 112(Pt. 3):329–338. [PubMed: 9885286]

Nakaso K, Kitayama M, Ishii T, Bannai S, Yanagawa T, Kimura K, Nakashima K, Ohama E, Yamada K. Effects of kainate-mediated excitotoxicity on the expression of rat counterparts of A170 and MSP23 stress proteins in the brain. Brain Res. Mol. Brain Res. 1999; 69:155–163. [PubMed: 10366737]

Nakaso K, Yoshimoto Y, Nakano T, Takeshima T, Fukuhara Y, Yasui K, Araga S, Yanagawa T, Ishii T, Nakashima K. Transcriptional activation of p62/A170/ZIP during the formation of the aggregates: possible mechanisms and the role in Lewy body formation in Parkinson's disease. Brain Res. 2004; 1012:42–51. [PubMed: 15158159]

Namkung Y, Sibley DR. Protein kinase C mediates phosphorylation, desensitization, and trafficking of the D2 dopamine receptor. J. Biol. Chem. 2004; 279:49533–49541. [PubMed: 15347675]

Neve KA, Seamans JK, Trantham-Davidson H. Dopa-mine receptor signaling. J. Recept. Signal Transduct. Res. 2004; 24:165–205. [PubMed: 15521361]

Park SK, Nguyen MD, Fischer A, Luke MP, Affar el B, Dieffenbach PB, Tseng HC, Shi Y, Tsai LH. Par-4 links dopamine signaling and depression. Cell. 2005; 122:275–287. [PubMed: 16051151]

Puls A, Schmidt S, Grawe F, Stabel S. Interaction of protein kinase C zeta with ZIP, a novel protein kinase C-binding protein. Proc. Natl Acad. Sci. USA. 1997; 94:6191–6196. [PubMed: 9177193]

Seibenhener ML, Babu JR, Geetha T, Wong HC, Krishna NR, Wooten MW. Sequestosome 1/p62 is a polyubiquitin chain binding protein involved in ubiquitin proteasome degradation. Mol. Cell. Biol. 2004; 24:8055–8068. [PubMed: 15340068]

Shin J. P62 and the sequestosome, a novel mechanism for protein metabolism. Arch Pharm Res. 1998; 21:629–633. [PubMed: 9868528]

Vadlamudi RK, Joung I, Strominger JL, Shin J. p62, A phosphotyrosine-independent ligand of the SH2 domain of p56lck, belongs to a new class of ubiquitin-binding proteins. J. Biol. Chem. 1996; 271:20235–20237. [PubMed: 8702753]

Wang X, Pal R, Chen XW, Kumar KN, Kim OJ, Michaelis EK. Genome-wide transcriptome profiling of region-specific vulnerability to oxidative stress in the hippocampus. Genomics. 2007; 90:201–212. [PubMed: 17553663]

Watts VJ, Neve KA. Sensitization of endogenous and recombinant adenylate cyclase by activation of D2 dopamine receptors. Mol. Pharmacol. 1996; 50:966–976. [PubMed: 8863843]

Whistler JL, Tsao P, von Zastrow M. A phosphorylation-regulated brake mechanism controls the initial endocytosis of opioid receptors but is not required for post-endocytic sorting to lysosomes. J. Biol. Chem. 2001; 276:34331–34338. [PubMed: 11443128]

Wooten MW, Seibenhener ML, Mamidipudi V, Diaz-Meco MT, Barker PA, Moscat J. The atypical protein kinase C-interacting protein p62 is a scaffold for NF-kappaB activation by nerve growth factor. J. Biol. Chem. 2001; 276:7709–7712. [PubMed: 11244088]

Worsley JN, Moszczynska A, Falardeau P, et al. Dopamine D1 receptor protein is elevated in nucleus accumbens of human, chronic methamphetamine users. Mol. Psychiatry. 2000; 5:664–672. [PubMed: 11126397]

Zatloukal K, Stumptner C, Fuchsbichler A, Heid H, Schnoelzer M, Kenner L, Kleinert R, Prinz M, Aguzzi A, Denk H. p62 Is a common component of cytoplasmic inclusions in protein aggregation diseases. Am. J. Pathol. 2002; 160:255–263. [PubMed: 11786419]

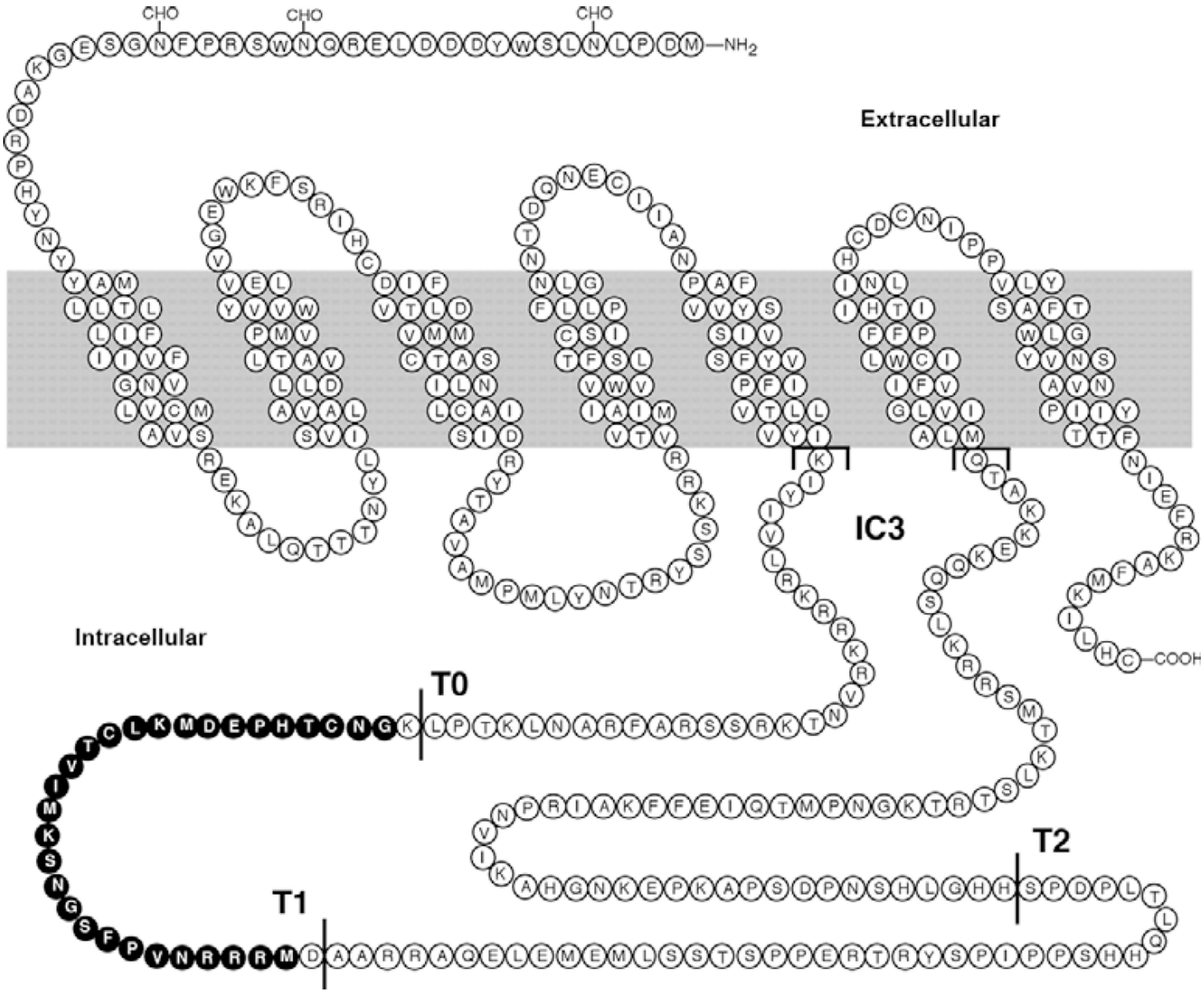

Fig. 1.

Membrane topography of the rat D_{2L} dopamine receptor. Solid circles represent amino acids that are absent in the D_{2S} receptor isoform. IC3 indicates the third cytoplasmic loop composed of residues Lys211–Gln374 (in brackets). For some yeast two-hybrid assays, three truncated versions of the IC3 loop were employed. T0 represents the IC3 fragment Lys211–Leu240, T1 represents the IC3 fragment Lys211–Asp271, and T2 represents the IC3 fragment Lys211–Ser311.

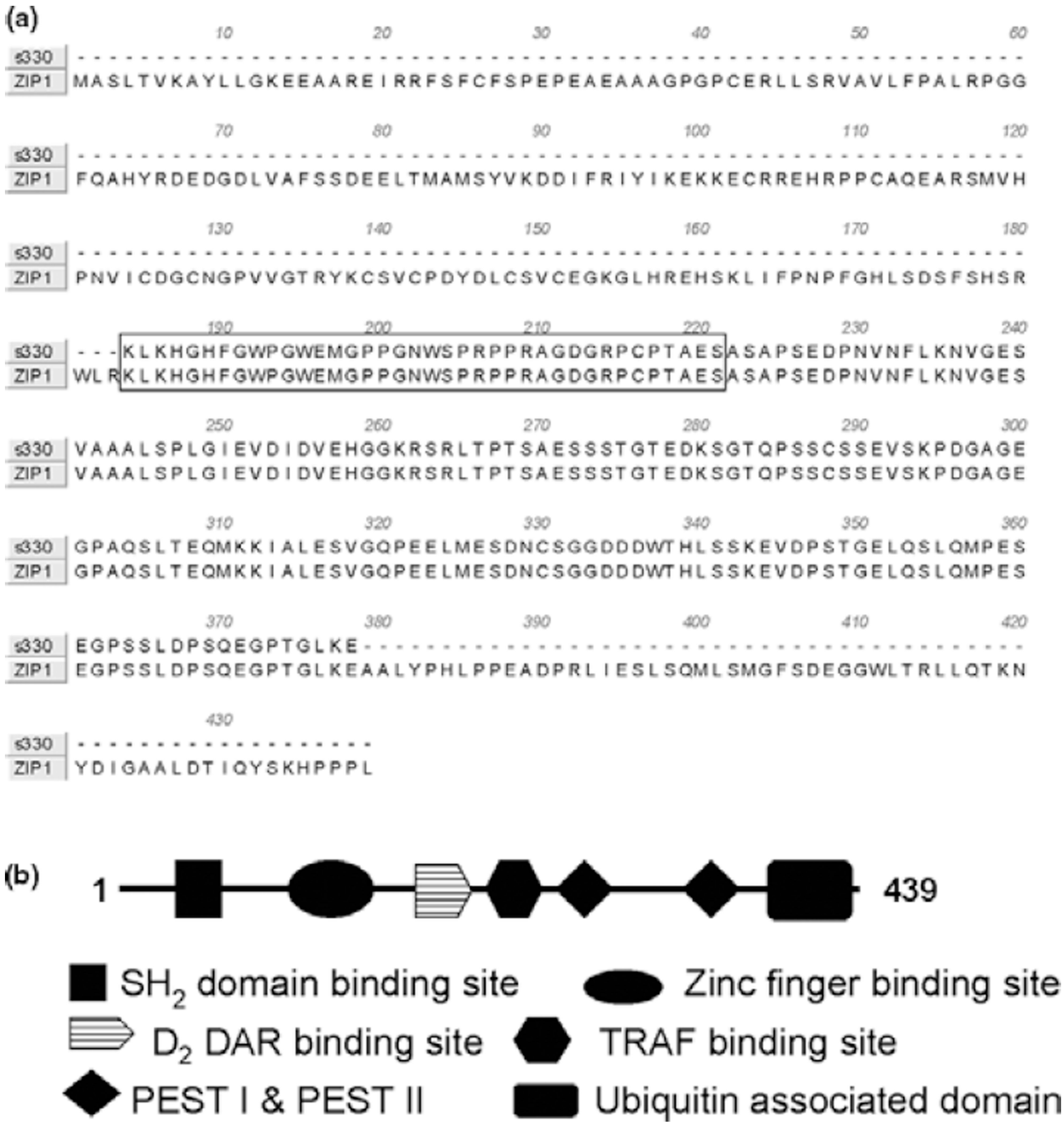

Fig. 2.

The alignment of ZIP1 and clone s330. (a) Clone s330 spans from K184 to E378 of ZIP. Proposed binding domain of ZIP1 to D_2 dopamine receptor is indicated in a box (see text). (b) Schematic diagram of ZIP protein. Six structural motifs of ZIP1: ■, an SH2 domain binding site; ⬬, a zz finger, zinc finger binding site; ⇒,, D_2 DAR binding site; ●,, a TRAF6 binding site (the ring-finger protein tumor necrosis factor receptor associated factor 6) and absent in ZIP2; ♦, PESTI and PESTII sites; ▬,, an ubiquitin-associated domain.

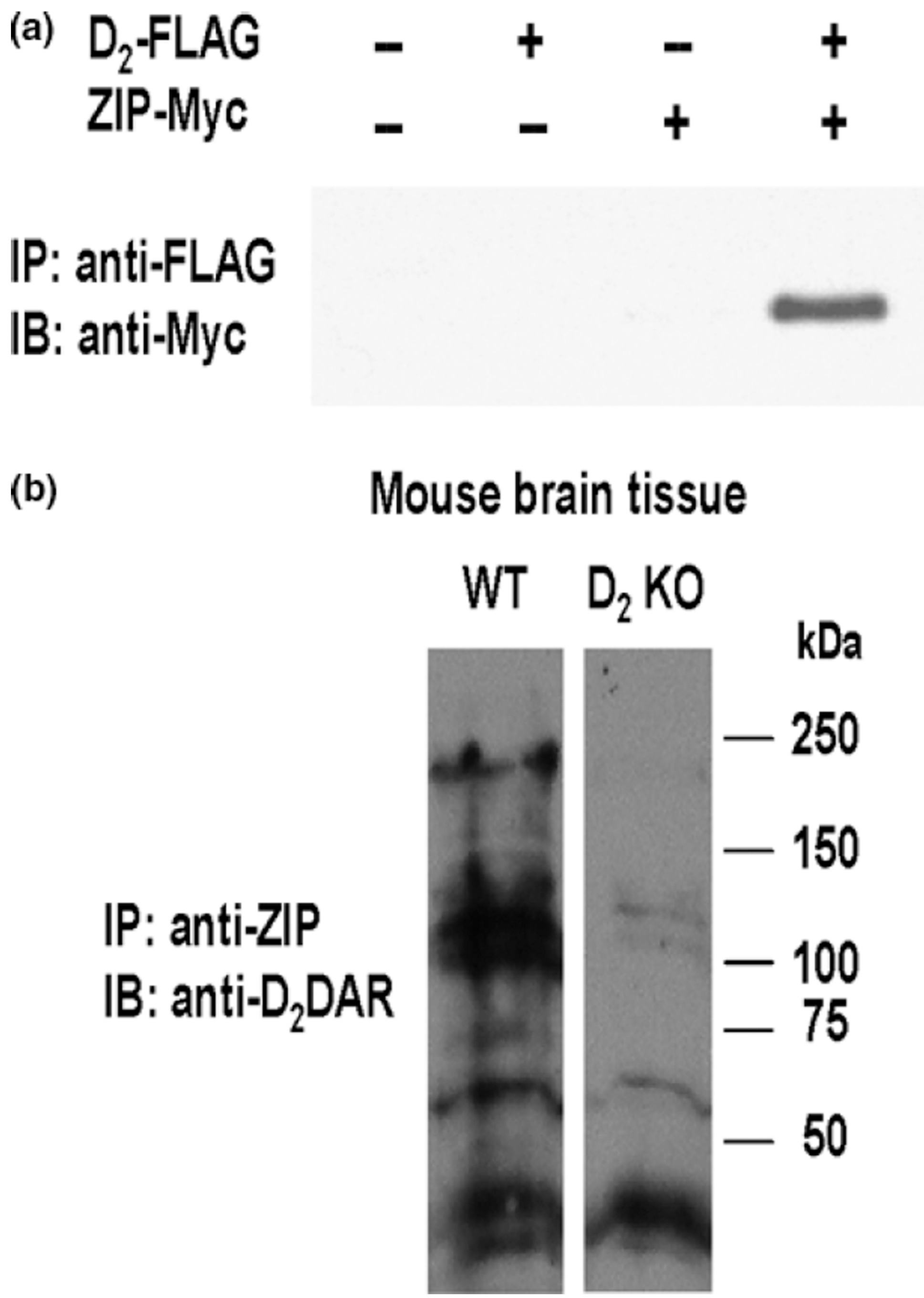

Fig. 3.

ZIP binds to D_2 DAR. (a) Co-immunoprecipitation from HEK293 cells. HEK293T cells were transfected with cDNA constructs tagged with FLAG (D_2 DAR) or Myc (ZIP). Forty-eight hours after transfection, cells were lysed and the immunoprecipitation assay was performed using anti-FLAG antisera as described in the Materials and methods. Western blot analysis was carried out with anti-Myc antibody conjugated with horseradish peroxidase. ZIP was detected in immunoprecipitates from cells transfected with both D_2 DAR and ZIP (lane 4), but not in cells with pcDNA (lane 1), D_2 DAR alone (lane 2), or ZIP alone (lane 3).

(b) Co-immunoprecipitation from mouse brain. The brains of wild-type and D_2 DAR knockout mice were homogenized in lysis buffer using a glass–glass homogenizer, sonicated for 1 min, and incubated in ice for an hour. The supernatants were saved and the immunoprecipitation assay using anti-ZIP antisera was performed as described in the Materials and methods. Western blot analysis was carried out with anti-D_2 DAR antibodies. Four proteins of ~250, 100, 75, and 55 kDa were detected only in brains from wild-type mice and appeared to be D_2 DAR oligomers/dimers and/or glycosylated D_2 DARs. All experiments were replicated three independent times with similar results.

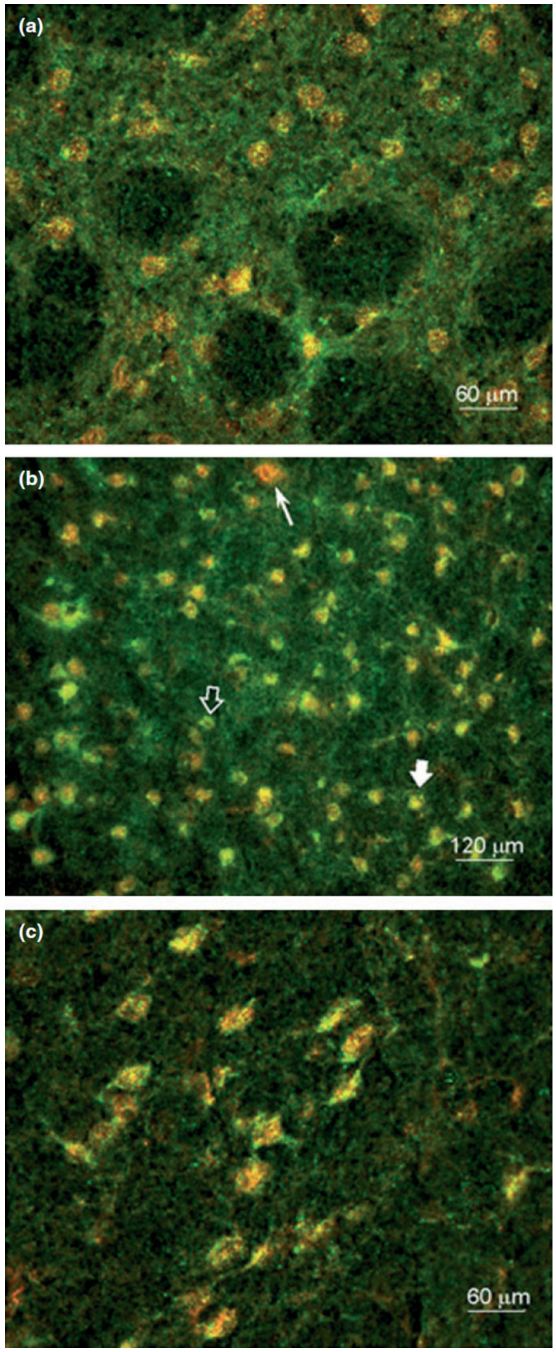

Fig. 4.

ZIP1 and the D_2 DAR are co-localized in brain. Immunofluorescent detection of ZIP (green label) and D_2 DAR (red label) staining was performed using fresh-frozen sections from rat brain regions as described in the Materials and methods. (a) Striatal tissue. (b) Somatosensory cortex. The pial surface is to the left in the image. (c) Higher magnification of the cortex. Calibration bars are indicated in each panel. All experiments were replicated three independent times with similar results.

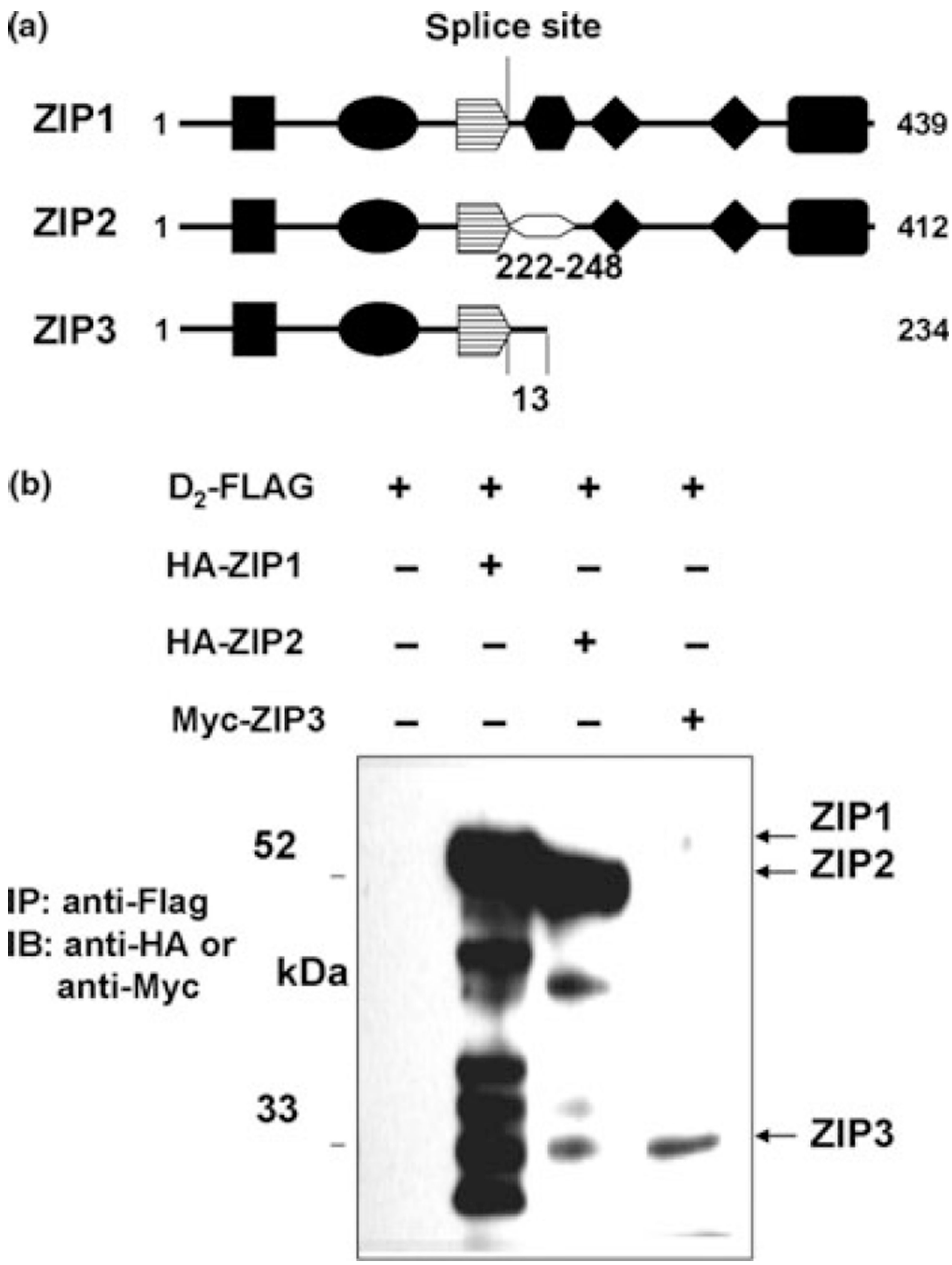

Fig. 5.

D_2 DAR binds all three splice variants for ZIP. (a) Schematic diagrams of three splice variants of ZIP: ZIP1, the longest form of ZIP; ZIP2, 27 amino acid sequences absent from the splice site of ZIP1 indicated by an open diamond; ZIP3, 218 amino acid sequences absent from the splice site of ZIP1 and the additional 13 amino acid sequences present from the splice site. (b) HEK293T cells were transfected with cDNA constructs, D_2 DAR-FLAG and ZIP1-HA, ZIP2-HA, or ZIP3-Myc. Forty-eight hours after transfection, cells were lysed and the immunoprecipitation assay was performed by incubating cell lysates with anti-

FLAG conjugated with agarose overnight in the cold room. Proteins bound to anti-FLAG antibody were separated by SDS–PAGE and transferred onto PVDF membranes. Western blot analysis was carried out with either anti-HA or anti-Myc antibody conjugated with HRP. All three splice variants, ZIP1, ZIP2, and ZIP3 were detected (lanes 1, 2, and 3, respectively). This experiment was replicated three independent times with similar results.

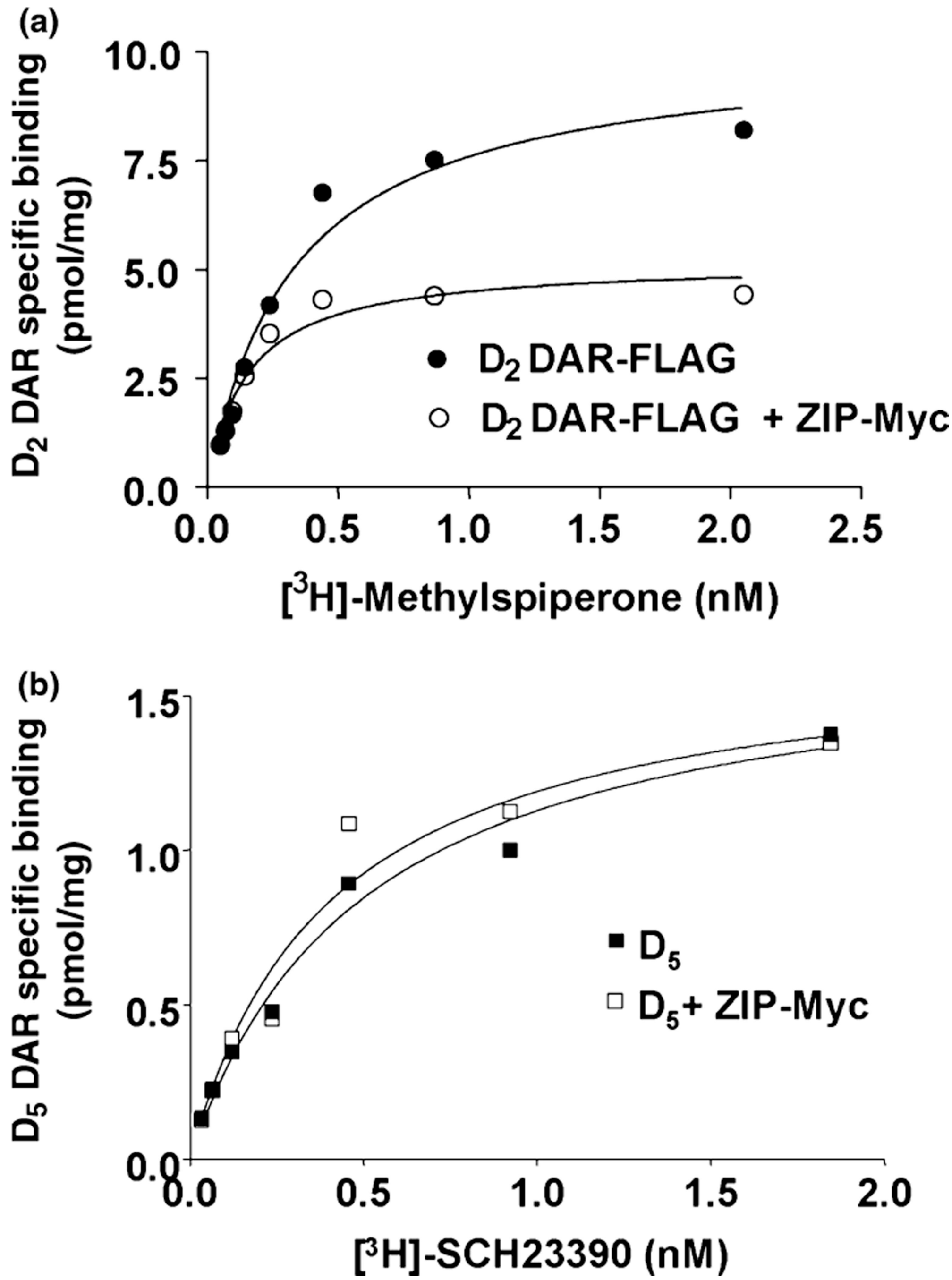

Fig. 6.

Effect of ZIP on D_2 DAR expression. (a) HEK293T cells were transfected with either D_2 DAR-FLAG alone or D_2 DAR-FLAG and ZIP-Myc expression vectors. Saturation radioligand binding assays in plasma membranes using the D_2-like DAR selective radioligand [^{3}H]methylspiperone were performed. The experiment shown for the D_2 DAR is representative of three such experiments. The binding parameters of this experiment are as follows: D_2 DAR, K_d = 0.3 nM, B_{max} = 10.2 pmol/mg; D_2 DAR + ZIP, K_d = 0.2 nM, B_{max} = 5.2 pmol/mg. (b) HEK293T cells were transfected with either D_5 DAR alone or D_5 DAR and ZIP-Myc expression vectors. Saturation radioligand binding assays in plasma membranes using the D_1-like DAR selective radioligand [^{3}H]SCH 23390 were performed. The experiment shown for the D_5 DAR is representative of three such experiments. The binding parameters of this experiment are as follows: D_5 DAR, K_d = 0.5 nM, B_{max} = 1.69 pmol/mg; D_5 DAR + ZIP, K_d = 0.4 nM, B_{max} = 1.67 pmol/mg.

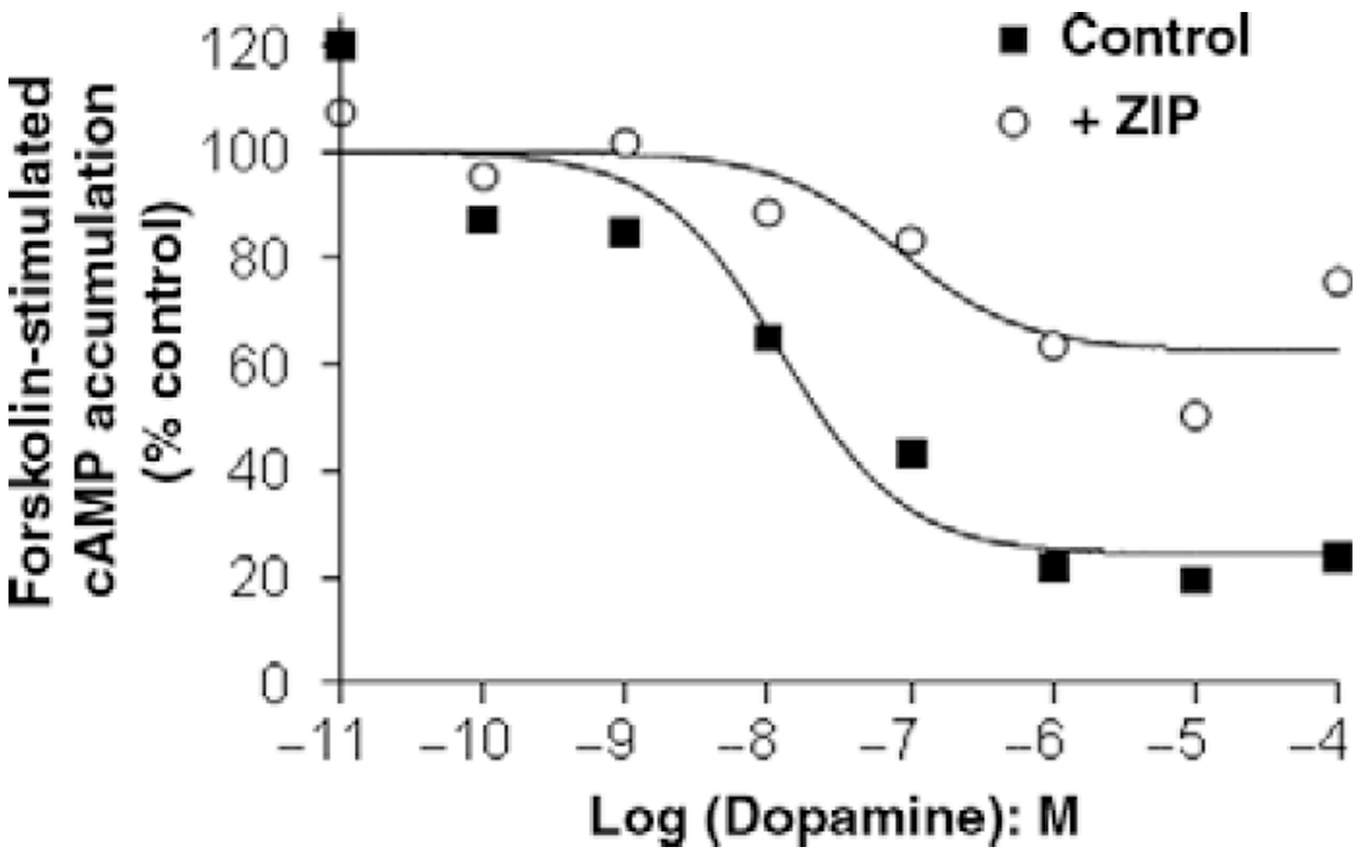

Fig. 7.

Dopamine inhibition of forskolin-stimulated cAMP accumulation. HEK293 cells were transiently transfected with D_2 DAR along with pcDNA (mock) or ZIP. After 48 h transfection, the cells were incubated with various concentrations of dopamine for 10 min in the presence of 3 μM forskolin, 30 μM Ro-20-1724 (phosphodiesterase inhibitor), 0.2 mM sodium metabisulfite (to prevent oxidation of dopamine), and 10 μM propranolol (to block endogenous β-adrenergic receptors) in 20 mM HEPES-buffered DMEM and then whole-cell cAMP assays were performed as described under Materials and methods. Data shown are from a single representative experiment, which was performed three times with similar results and expressed as percent inhibition of forskolin-stimulated cAMP accumulation. The estimated EC_{50} parameter was 12.4 nM for D_2 DAR and 84.2 nM for D_2 DAR + ZIP1.

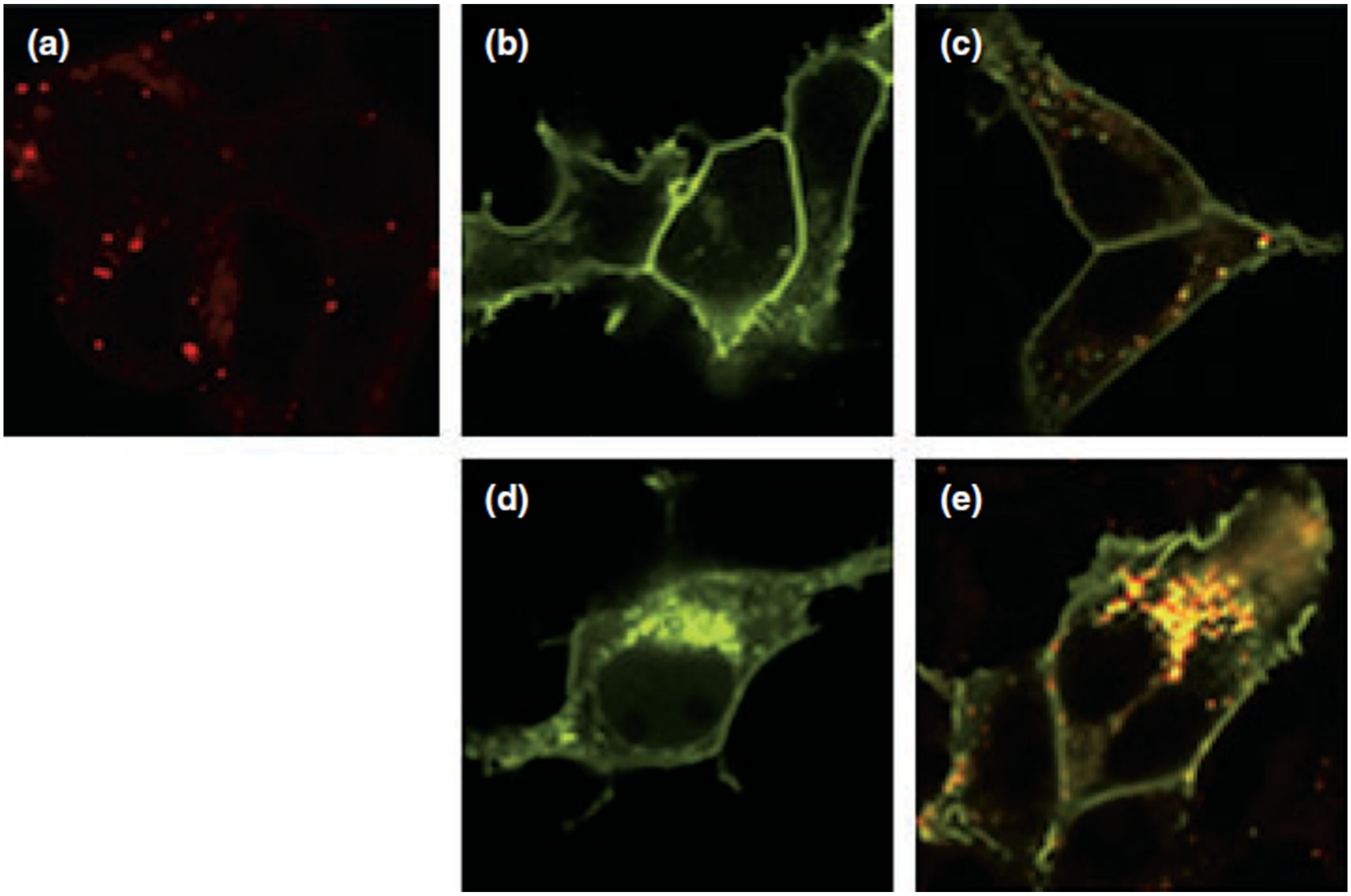

Fig. 8.

Effect of ZIP on D_2 DAR tracking to lysosomes. HEK293T cells were transfected with either empty pcDNA vector, D_2-YFP, and/or ZIP as described in the Materials and methods. On the day of the experiment, the cells were reseeded in 35 mm glass-bottomed plates and were incubated with or without 75 μM LysoTracker Red for 90 min. The cells were then visualized via confocal microscopy for the distribution of receptor (green) and/or LysoTracker Red (red). Co-localization is shown in *yellow*. (a) pcDNA transfected cells were treated with LysoTracker Red only. (b) Cells expressing D_2-YFP only. (c) Cells expressing D_2-YFP and treated with LysoTracker Red. (d) Cells expressing D_2-YFP and ZIP. (e) Cells expressing D_2-YFP and ZIP and treated with LysoTracker Red.

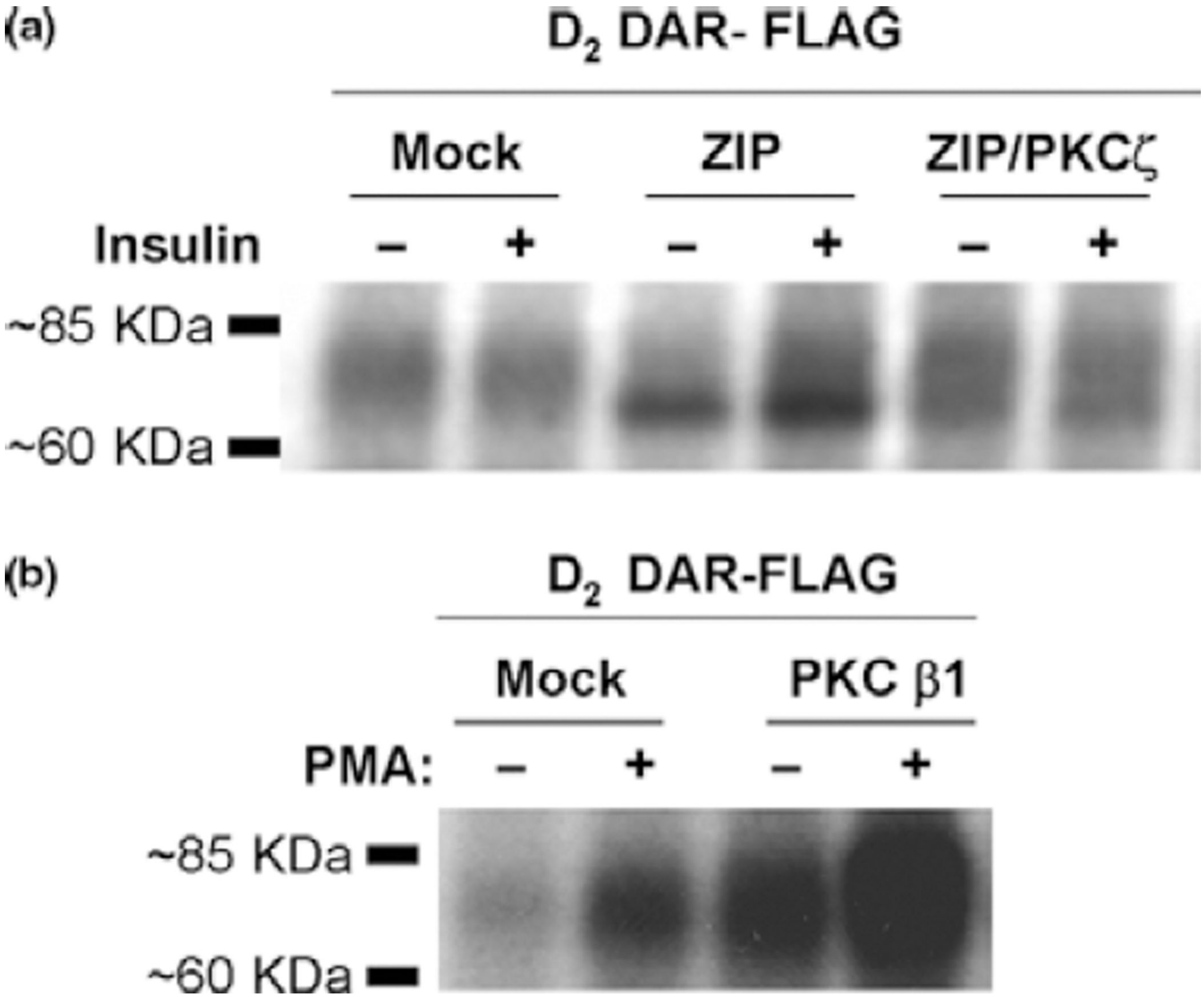

Fig. 9.

The effect of over-expression of ZIP along with PKCζ on D_2 DAR phosphorylation. HEK293T cells were transiently transfected with the FLAG-tagged D_2 DAR along with either pcDNA (mock), ZIP1, ZIP1 and PKCζ, PKCβ1 as indicated. [$^{32}PO_4$]-labeled cells were incubated with or without 100 nM insulin (a) or 1 μM phorbol-12-myristate-13-acetate (PMA) (b) for 20 min and then solubilized. The samples were then subjected to immunoprecipitation as described under Materials and methods. Receptors were quantified and equal amounts of receptor protein were loaded into each gel lane and resolved by 4–20% SDS–PAGE. The extent of receptor phosphorylation was visualized by autoradiography. The data shown are representative from four independent experiments.

Table 1

Yeast two-hybrid interaction of ZIP/s330 clone with third cytoplasmic domains from all dopamine receptors

	Gal/Raf-H-U-W-L	Gal/Raf-H-U-W, X-Gal
Dopamine receptors	**ZIP/s330**	**ZIP/s330**
D_1	No	0
D_{2L}	Yes	4
D_2T0	No	0
D_2 T1	Yes	4
D_2 T2	Yes	4
D_3	No	0
D_4	No	0
D_5	No	0
Lex A	No	0
Positive control	Yes	4

The EGY48 yeast strain was sequentially transformed with a LacZ reporter vector and bait vectors containing third cytoplasmic loops from each dopamine receptor as indicated. Yeast two-hybrid analyses were subsequently carried out as described in the Materials and methods. The bluest reactionis rated 4. ZIP, protein kinase C-ζ interacting protein.